

CCE: Sample Efficient Sparse Reward Policy Learning for Robotic Navigation via Confidence-Controlled Exploration

Bhrij Patel¹, Kasun Weerakoon¹, Wesley A. Suttle², Alec Koppel³,
Brian M. Sadler⁴, Tianyi Zhou¹, Amrit Singh Bedi⁵, and Dinesh Manocha¹

Abstract—We introduce Confidence-Controlled Exploration (CCE), a novel exploration scheme designed to enhance the training sample efficiency of reinforcement learning (RL) algorithms for sparse reward settings such as robot navigation. Sparse rewards are common in RL and convenient to design and implement, but typically hard to deal with due to the challenges of exploration. Existing methods deploy regularization-based methods to deal with the exploration challenges. However, it is hard to characterize the balance between exploration and exploitation because regularization modifies the reward function itself, hence changing the objective we are optimizing for. In contrast to regularization-based approaches in the existing literature, our approach, CCE, is based on a novel relationship we provide between gradient estimation and policy entropy. CCE dynamically adjusts the number of samples of the gradient update used during training to control exploration. Interestingly, CCE can be applied to both existing on-policy and off-policy RL methods, which we demonstrate by empirically validating its efficacy on three popular RL methods: REINFORCE, Proximal Policy Optimization (PPO), and Soft Actor-Critic (SAC) for goal-reaching robotic navigation tasks. We demonstrate through simulated and real-world experiments that CCE outperforms conventional methods that employ constant trajectory lengths and entropy regularization when constraining the sample budget. For a fixed sample budget, CCE achieves an 18% increase in navigation success rate, a 20-38% reduction in navigation path length, and a 9.32% decrease in elevation costs. Furthermore, we showcase the versatility of CCE by integrating it with the Clearpath Husky robot, illustrating its applicability in complex outdoor environments.

I. INTRODUCTION

Reinforcement learning (RL) [1] is an important component of learning in robotic systems in a wide variety of complex domains, including search-and-rescue [2], disaster relief [3], and planetary exploration [4] applications. However, traditional RL methods often hinge on the availability of a dense reward structure [5], which may rarely be available in complex, unpredictable environments [6]–[9]. Thus, reward function sparsity [10] frequently arise when applying RL methods to robotics problems, such as robotic navigation, due to its simplicity to implementation and lack of need for

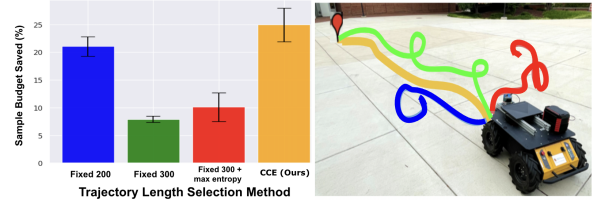


Fig. 1: Robot navigation using policies trained with the REINFORCE policy gradient algorithm using four trajectory length schemes. We compare three fixed trajectory lengths, 200 (blue), 300 (green), and 300 with max entropy regularization (red), against CCE (ours) (yellow) in real-world environments. More details can be found in Sec. IV. The drawn trajectories are sample representations of the robot’s odometry data collected. CCE enhances training sample efficiency (shown in the figure by the lower value of the orange bar plot) by adaptively varying trajectory length. CCE results in better navigation policies compared to baseline approaches and generates shorter and more successful test-time trajectories.

expert knowledge to design required dense reward structures. However, this simplicity comes with a sparse feedback signal to learn from, thus leading to a limited exploration of the environment, and to a premature exploitation of a suboptimal policy [11]. Existing literature in RL for robotics in sparse rewards has utilized methods such as entropy regularization [12], reward shaping [13]–[16], curiosity-driven exploration [5], [17]. However, these methods are regularization-based that change the reward optimization objective which can lead to instability in learning [6].

Another major challenge of existing works comes from the sample inefficiency of exploration in sparse rewards. This issue is significant in robotic systems, due to the simulation-intensive nature of RL methods and the high computational associated with realistic robotics simulation platforms [18]. Thus, RL training typically requires finding an optimal policy in a constrained sample budget. In this work, we propose an exploration paradigm to respect the practicality of limited training samples. We achieve this by *balancing* exploration, rather than *encouraging* it through a novel connection between the parameterized policy’s *confidence* and its gradient estimation.

Main Contributions: We present Confidence-Controlled Exploration (CCE), a general technique for improving the sample efficiency of RL methods for robotics navigation tasks with minimal modifications to the existing state-of-the-art methods. Our method leverages policy confidence, measured by the average conditional policy entropy across all states, to regulate exploration. Specifically, we focus on balancing exploration with policy entropy by adaptively adjusting a key feature in most RL methods: trajectory length, defined as the number of samples the robot collects in

¹Department of Computer Science, University of Maryland, College Park, MD, USA. Emails: {bbpl3, kasunw, tianyi, dmanocha}@umd.edu

²U.S. Army Research Laboratory, Adelphi, MD, USA. Email: wesley.a.suttle.ctr@army.mil

³JP Morgan AI Research, New York, NY, USA. Email: alec.koppel@jpmchase.com

⁴University of Texas at Austin, Austin, TX, USA. Email: brian.sadlerf@ieee.org

⁵Department of Computer Science, University of Central Florida, Orlando, FL, USA. Email: amritsingh.bedi@ucf.edu

This work was supported by Army Cooperative Agreement W911NF2120076. We acknowledge the support of the Maryland Robotics Center and Northrup Grumman Seed Grant 2022.

the environment before each gradient update during training. For navigation tasks, a data sample refers to any action the mobile robot takes at a given state, the resulting state transition in the environment, and the corresponding reward.

To design CCE, our novel approach connects the need for the policy to explore to the *mixing time* of the policy. The mixing time of a policy is the amount of time it takes for a robot to reach its limiting behavior under that policy. When mixing time is large, ensuring that trajectories are sufficiently long is important for obtaining accurate estimates of system behavior and algorithmic essentials, such as policy gradients [19]. Conversely, when mixing time is short, keeping trajectory lengths proportional to it frees up resources for faster policy updates and more efficient exploration of the environment. Unfortunately, mixing time is typically difficult to estimate in complex environments [20], [21], so proxy methods for determining trajectory length are needed. In this work, we utilize a previously unexplored connection between a policy’s mixing time and its policy entropy to formulate CCE. We increase the sample efficiency by adaptively tuning the trajectory length required to update the policy parameter, thus decreasing the number of samples needed to learn an optimal policy for navigation tasks. Our results include:

- We empirically establish a positive correlation between the policy entropy and the spectral gap of its induced Markov chain. We show that this correlation is present with various transition dynamics. This insight motivates our use of the changing policy entropy to control the amount of exploration during training.
- We take advantage of this empirical insight by utilizing a monotonic mapping between policy entropy and trajectory length to facilitate exploration with sparse rewards and serve as the foundation for CCE.
- We present extensive empirical results using multiple RL methods, including REINFORCE [22] and Proximal Policy Optimization (PPO) [23] and Soft Actor-Critic (SAC) [12], to show that CCE improves the sample efficiency with both on-policy and off-policy methods. Furthermore, by showing results on SAC, we show that CCE also improves sample efficiency for algorithms that employ entropy regularization. Our experiments in goal-reaching navigation tasks with both even and uneven terrains demonstrate that CCE outperforms constant trajectory length and exploration encouragement methods, with constrained samples.
- We evaluate the navigation performance of CCE in both simulated and real-world outdoor environments using a Clearpath Husky robot. We observe that, for a fixed, *limited* sample budget, CCE leads to an 18% increase in navigation success rate, a 20-38% decrease in the navigation path length, and a 9.32% decrease in the elevation cost compared to the policies from baselines.

A. Related Works

Sparse Rewards: For model-free reinforcement learning, reward sparsity greatly affects policy search [5], [24] as a mobile robot will rarely receive any feedback to adjust its behavior. To produce more rewards which the algorithm can learn from, reward-shaping methods based on intrinsic rewards have been proposed. Methods in [13] and [25]

modified the reward output to encourage exploration of the environment. Furthermore, [26] and [27] formulated a heavy-tailed policy to encourage exploration in sparse environments. Prior work used imitation learning and demonstration [15], [28] and curriculum learning [29] to overcome the challenges of sparse rewards.

Exploration and Exploitation in RL and Navigation:

To balance exploration and exploitation, prior work has used the uncertainty of a surrogate cost function estimation from the visual field of view [30] and a world model in model-based RL [31], [32]. In motion planning, [33] introduced a planner that balances exploration and exploitation using explicit information on the environmental information. By connecting exploration to policy gradient estimation, our approach, CEE, is agnostic to data modality and does not require a world model or any explicit information on the given environment. Exploration-exploitation for multi-robot systems was considered in [34]–[36].

RL for Navigation: Motion planning and navigation has been well studied in robotics [37]–[39]. RL-based methods have been extensively used for robot navigations [40]. Methods such as in [41] used DRL to find reliable paths for outdoor navigation, while [42] learned a global map to find the shortest path out of a maze with RL. In [43], classical methods were used to create a hierarchical RL approach.

II. PROBLEM FORMULATION

A. Reinforcement Learning and Policy Gradient Methods

We consider a Markov Decision Process (MDP) characterized by the tuple $\mathcal{M} := (\mathcal{S}, \mathcal{A}, \mathbb{P}, r)$, where \mathcal{S} is the state space for the robot in the environment, \mathcal{A} is the set of possible actions the robot can take, \mathbb{P} is the transition probability kernel that determines the next state $s' \in \mathcal{S}$ given $s \in \mathcal{S}, a \in \mathcal{A}$ via $s' \sim \mathbb{P}(\cdot|s, a)$, and $r : \mathcal{S} \times \mathcal{A} \rightarrow [0, r_{\max}]$ is the reward function. The mobile robot navigates through this environment using a (potentially stochastic) policy π that provides a conditional probability distribution over actions a given a state s . Given a policy π and transition kernel \mathbb{P} , the transition dynamics of the ergodic Markov chain induced by π over \mathcal{M} is given by $\mathbb{P}_{\pi}(s'|s) = \sum_{a \in \mathcal{A}} \mathbb{P}(s'|s, a)\pi(a|s)$. The goal in the RL setting is to find a policy maximizing long-run reward over \mathcal{M} . To achieve this, let μ be the unique stationary distribution to the ergodic Markov Chain. Thus, one infinite-horizon objective typically considered in the RL literature is the expected discounted reward given by

$$J(\pi) = \mathbb{E}_{s \sim \mu, a \sim \pi} \left[\sum_{t=0}^{\infty} r(s_t, a_t) \right], \quad (1)$$

In (1), the expectation is over the policy and initial state distributions. In the average-reward settings, the state-action value function corresponding to a given policy π is defined by $Q_{\pi}(s, a) = \mathbb{E}_{\pi} [\sum_{t=0}^{\infty} r(s_t, a_t) - J(\pi) \mid s_0 = s, a_0 = a]$.

Policy Gradient Algorithm. To handle large, potentially continuous state and action spaces, we focus on the case where policy π is parameterized by a vector $\theta \in \mathbb{R}^d$, where d denotes the parameter dimension, leading to the notion of a parameterized policy π_{θ} . We define $J(\theta) = J(\pi_{\theta})$. Then, following policy gradient theorem [44], we note that

$$\nabla J(\theta) = \mathbb{E}_{\pi_{\theta}, \mu} [Q_{\pi}(s, a) \nabla \log \pi_{\theta}(a|s)], \quad (2)$$

which provides the gradient expression to perform gradient ascent on the objectives $J(\theta)$. At update u the policy gradient estimate is obtained by generating a $K \in \mathbb{N}$ length trajectory $\tau_t := \{s_0, a_0, \dots, s_{K-1}, a_{K-1}\}$ using π_{θ_u} , and then computing

$$\widehat{\nabla J(\theta_u)} = \frac{1}{K-1} \sum_{k=0}^{K-1} r(s_k, a_k) \nabla \log \pi_{\theta_t}(a_k | s_k). \quad (3)$$

This expression is then used to perform a gradient update of the form $\theta_{u+1} = \theta_u + \eta \widehat{\nabla J(\theta_u)}$, for some stepsize $\eta > 0$. In REINFORCE, increasing K , and therefore the overall number of samples naturally improves the quality of the estimator given in Equation (3) [45]. However, in reinforcement learning for robotic navigation, simulation data to train mobile agent can be expensive to obtain or generate. Thus, reducing the number of training samples needed without degrading navigation performance is crucial in mitigating operation costs. In the next section, we will explain mixing time and its importance to gradient estimation.

B. Mixing Time and Spectral Gap

In policy gradient algorithms an important issue is that, to obtain good estimates of the expectation in (2), which is taken with respect to the stationary distribution, μ_θ , induced over the underlying MDP by π_θ , longer trajectories are often needed. The length of the trajectories is dictated by the mixing time – to be defined below – of the associated policy. Recent work on stochastic optimization [46] and policy gradient (PG) methods [19] has highlighted and clarified the connection between Markov chain mixing time and ideal trajectory length, which we will later use to connect confidence to exploration.

We assume throughout that, for a given policy parameter θ , the Markov chain induced by π_θ on the MDP \mathcal{M} is ergodic, which is a common assumption in theoretical analyses of RL methods [19], [46]–[48]. First note that the ergodicity assumption guarantees that the Markov chain has a unique stationary distribution μ_θ . For an MDP $\mathcal{M} = (\mathcal{S}, \mathcal{A}, \mathbb{P}, r)$ and policy π_θ , the ϵ -mixing time of π_θ is $\tau_{mix}^\theta(\epsilon) := \inf\{t : \sup_{s \in \mathcal{S}} \|\mathbb{P}_{\pi_\theta}^t(\cdot | s) - \mu_\theta(\cdot)\|_{TV} \leq \epsilon\}$. By convention, the mixing time is defined as $\tau_{mix}^\theta := \tau_{mix}^\theta(1/4)$ [47].

Though mixing times are useful in determining trajectory lengths, they are difficult to estimate in practice. Therefore, an alternative is estimating a lower bound. One such quantity that can lower bound of mixing time is the absolute spectral gap, or simply spectral gap, of the induced transition matrix \mathbb{P}_{π_θ} , $1 - \lambda_2^\theta$, where λ_2^θ is the second largest eigenvalue of \mathbb{P}_{π_θ} , as stated in the theorem below [49]:

Theorem 2.1: Let τ_{mix}^θ be the mixing time induced by policy π_θ . Then,

$$\tau_{mix}^\theta(\epsilon) \geq \mathcal{O}\left(\frac{1}{1 - |\lambda_2^\theta|}\right). \quad (4)$$

When an estimate of \mathbb{P}_{π_θ} is available, this provides a method for bounding its mixing time. Unfortunately, estimating \mathbb{P}_{π_θ} is impractical in large and complex state and action spaces [20], [21]. Thus, a proxy for the spectral gap is crucial for navigation in complex environments. In the following section, we leverage this theorem to empirically establish a

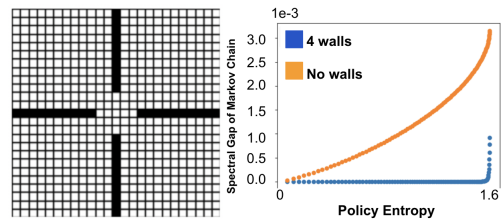


Fig. 2: [LEFT] Visualization of 25×25 gridworld with 4 walls (black) dividing it into equal regions. [RIGHT] Positive correlation between a policy’s entropy and the spectral gap of its induced transition matrix over two different gridworld environments. Policy entropy is a viable proxy for mixing time.

useful connection between policy entropy and spectral gap to control the exploration with no need to estimate \mathbb{P}_{π_θ} .

III. PROPOSED APPROACH: CONTROLLED EXPLORATION-BASED POLICY LEARNING

A. Key Insight: Policy Entropy as a Proxy for Mixing Time

Given a policy π_θ , we would ideally like to base trajectory length for our PG updates on the spectral gap $1 - \lambda_2^\theta$ that lower bounds τ_{mix}^θ . However, without prior knowledge of the transition kernel \mathbb{P} of the underlying MDP, it is difficult to calculate the spectral gap of the induced transition matrix, \mathbb{P}_{π_θ} . One possible workaround is to estimate the transition kernel, but this quickly becomes intractable due to the $\Omega(|\mathcal{S}||\mathcal{A}|)$ number of samples required for each estimate.

Interestingly, one key insight we observe in 25-by-25 gridworld environments is that if the policy entropy decreases, the spectral gap of the induced transition matrix also decreases or stays the same (Figure 2).

Remark: We have not trained any agent to navigate in the gridworld. We have a static environment where we manually designed transition kernel matrices and multiplied each one with 100 different tabular policies with various entropies, from uniform distributions to deterministic, distributions to estimate the underlying Markov Chains and their corresponding spectral gaps. Because of the impracticality of calculating spectral gaps from more complex environments, we provide these proof-of-concept experiments with gridworld environments to support the formulation of our CCE approach.

As previously mentioned, we define the policy entropy in the discrete action space case as average the Shannon entropy [50] over the state space:

$$H(\pi_\theta) = -\frac{1}{|\mathcal{S}|} \sum_{s \in \mathcal{S}} \sum_{a \in \mathcal{A}} \pi_\theta(a|s) \log \pi_\theta(a|s). \quad (5)$$

In the continuous action space case for the robotic navigation experiments in Section IV, we use the closed-form differential entropy for a multivariate Gaussian distribution,

$$H(\pi_\theta) = -\frac{1}{|\mathcal{S}|} \sum_{s \in \mathcal{S}} \frac{1}{2} \log((2\pi e)^N \det(\Sigma_\theta(s))). \quad (6)$$

where N is the action space dimension and $\Sigma_\theta(s)$ is the covariance matrix of the policy $\pi_\theta(\cdot|s)$. We note that there are no analytical equations to calculate mixing time, and calculating spectral gap requires knowledge of the transition dynamics $P(s'|s, a)$ in the form of a matrix, which is infeasible for complex environments. Thus, using analytical

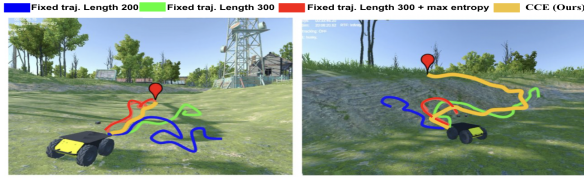


Fig. 3: Comparison of four different trajectory-length schemes on [LEFT] even and [RIGHT] uneven terrain navigation tasks in Unity-based outdoor robot simulator. For REINFORCE, PPO, and SAC, using CCE as the trajectory length scheme for 150 episodes leads to a policy with a shorter path length return than baselines with limited samples. The drawn trajectories are sample representations of the robot’s odometry data collected. The trajectories pictured are representative of all 3 algorithms since we found that each trajectory-length scheme leads to similar navigation regardless of the RL algorithm. See Figures 4 and 6 for training details.

Equations (5) and (6) as a proxy for mixing time is a simple method that can be used for model-free or model-based RL.

B. CCE: Confidence-Controlled Exploration

We now present our novel CCE approach for robotic navigation. The key to our approach is to select trajectory length based on the current value of the policy entropy, our measure for confidence. We perform this computation using a monotonic mapping f from the range of possible policy entropy values to a range of possible trajectory length values. In this paper, we utilize a linear function; however, we note that f can be implemented with any monotonic mapping such as an exponential function. Let H_i denote the maximum possible policy entropy value and H_c the policy entropy of the current policy. In practice, we choose $H_i = H(\pi_{\theta_0})$ to be the entropy of the initial policy, since policy entropy tends to decrease during training. Let $K_i \in \mathbb{N}$ denote the user-specified initial trajectory lengths and let $\alpha > 0$ denote a user-specified sensitivity parameter that controls the rate of change of length. For our experiments, we determine the trajectory length, K_c , corresponding to H_c using the mapping f below:

$$K_c = f_{K_i, \alpha}^{H_i}(H_c) = \text{round} \left(\alpha - \frac{H_c}{H_i}(\alpha - K_i) \right), \quad (7)$$

where the rounding operation is to ensure that K_c is always an integer. Furthermore, in our experiments, we initialize our policies with a Gaussian distribution. To ensure, that H_c never increases too much so that K_c becomes 0, one can initialize with a uniform distribution so that H_i is the maximum possible entropy. Algorithm 1 summarizes our CCE methodology for adaptive trajectory length PG methods. Note that any on-policy PG method can be used to carry out the policy gradient update in line 3. The training is divided into episodes where the start location and goal are constant between episodes. During each episode, a gradient update occurs after every trajectory. The episode ends when the goal is reached or when a user-set number T of interactions has occurred. For clarification, given an episode, the trajectory length is fixed. K_c is only adjusted based on the policy entropy at the start of the new episode.

IV. EXPERIMENTS AND RESULTS

RL Algorithms. We choose three RL algorithms to integrate CCE into for improved sample efficiency: REIN-

Algorithm 1 Policy Learning with CCE

- 1: **Initialize:** policy parameter θ_0 , policy entropy H_i , trajectory length K_i , current trajectory length $K_c = t_i$, number of episodes E , maximum number T of iterations per episode, sensitivity parameter α , update index $u = 0$
 - 2: **for** $e = 0, \dots, E - 1$ **do**
 - 3: calculate H_c using 5 for discrete actions, 6 for continuous actions
 - 4: calculate K_c using 7
 - 5: $t = 0$
 - 6: **while** $t < T$ **do**
 - 7: collect trajectory
 $\mathcal{T} = (s_1, a_1, r_1), \dots, (s_{K_c}, a_{K_c}, r_{K_c})$ using π_{θ_u}
 - 8: **Perform** gradient update using \mathcal{T} to obtain θ_{u+1}
 - 9: $t = t + K_c$
 - 10: $u = u + 1$
 - 11: **end while**
 - 12: **end for**
 - 13: **Return:** π_{θ_u}
-

FORCE, PPO, and SAC. As REINFORCE and PPO are both on-policy policy gradient methods and SAC is an off-policy method, we show that CCE can improve the sample efficiency of various classes of policy gradient algorithms. For PPO and SAC, we adaptively change the size of the replay buffer. For information on hyperparameters, such as network architecture, K_i , and α , please see the Appendix.

Baselines. Since our proposed approach relies on adaptive trajectory length, for each algorithm we test CCE with, we compare it against the same algorithm with fixed trajectory lengths. We also compare with fixed trajectory lengths with max-entropy regularizer as that encourages exploration.

We also incorporate a classical navigation algorithm Ego-graph [51], to highlight the navigation performance of our method under challenging terrain conditions. Ego-graph is a baseline method in [51] that utilizes elevation data to obtain the actions that minimize the elevation gradient cost.

Environments: We utilize two environments in a unity-based outdoor robot simulator. Finally, we deploy navigation policies trained for a fixed sample budget using the robot simulator on a real Clearpath Husky robot. We present the details of the training environments below:

Simulated Even and Uneven Terrain Navigation: We use a Unity-based outdoor simulator with a Clearpath Husky robot model to train policies for two navigation tasks: 1. Goal Reaching, 2. Uneven terrain navigation using the Reinforce algorithms. The Unity simulator includes diverse terrains and elevations for training and testing. We restrict ourselves to a $100m \times 100m$ region during training. We used identical policy distribution parameters and neural network architectures with all four algorithms during training and evaluation. The policies are trained using Pytorch in the simulator equipped with a Clearpath Husky robot model, and a ROS Melodic platform. The training simulations are executed on a workstation with an Intel Xeon 3.6 GHz CPU and an Nvidia Titan GPU.

Our agent is a differential drive robot with a two-dimensional continuous action space $a = (v, \omega)$ (i.e. linear

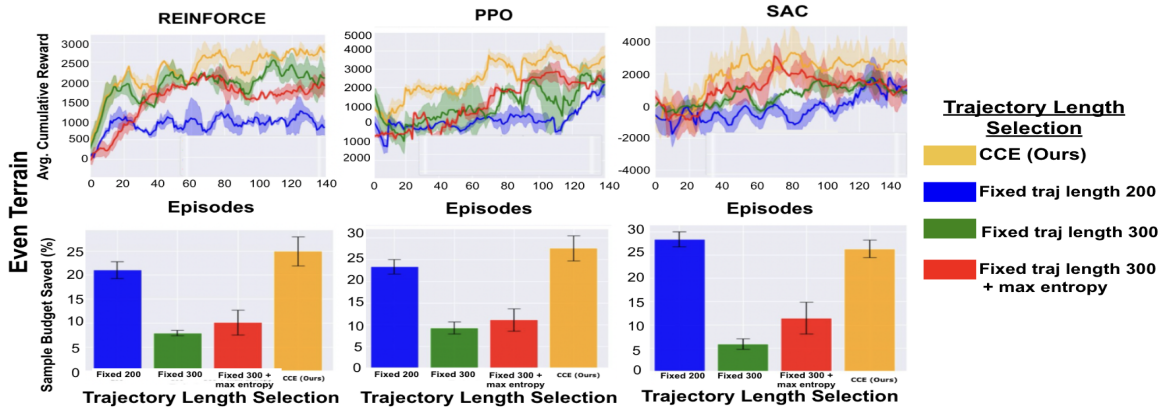


Fig. 4: [TOP] Learning curves during training and [BOTTOM] percent of sample budget ($\sim 4.5e4$) saved during navigation tasks for the even terrain (left of Figure 3). Comparison of [LEFT] REINFORCE, [MIDDLE] PPO, and [RIGHT] SAC, with constant and adaptive trajectory lengths. For each algorithm, CCE converges to a higher cumulative reward while expending less of the total budget. We ran 8 to 10 independent replications for each of the 12 experiments. Although a fixed trajectory length of 200 saves the sample budget comparably to CCE, it achieves lower reward in all cases due to the robot flipping over thus causing episodes to end.

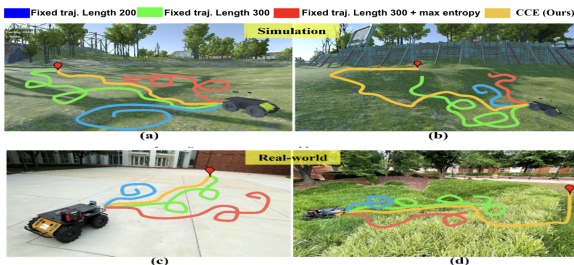


Fig. 5: Sample navigation trajectories generated in simulated (a, b) and real-world (c, d) environments by policies trained with REINFORCE using CCE vs. fixed trajectory lengths at a fixed sample budget of $\sim 4.5e4$. We observed that the fixed trajectory length policies often fail at test time due to inefficient use of the available sample budget during training. In contrast, CCE policies successfully complete the tasks after training with the same limited sample budget. The experiments with a real Clearpath Husky robot validate that CCE can be transferred onto real robotic systems without significant performance degradation. The drawn trajectories are sample representations of the robot’s odometry data collected during each task.

and angular velocities). The simulator includes even and uneven outdoor terrains and the state space varies for the two navigation tasks and is obtained in real-time from the simulated robot’s odometry and IMU sensors. The state inputs used in the two scenarios are,

- $d_{goal} \in [0, 1]$ - Normalized distance (w.r.t the initial straight-line distance) between the robot and its goal;
- $\zeta_{goal} \in [0, \pi]$ - Angle between the robot’s heading direction and the goal;
- $(\phi, \theta) \in [0, \pi]$ - Roll and pitch of robot, respectively.

Inspired by [26], we define three reward functions to formulate the sparse rewards to train our navigation policies: Goal distance reward r_{dist} , Goal heading reward r_{head} , and Elevation reward r_{elev} to formulate the sparse rewards to train our navigation policies. Hence, $r_{dist} = \frac{\beta}{2}\mathcal{N}(d_{goal}, \sigma^2) + \beta\mathcal{N}(0, \sigma^2)$ and $r_{head} = \mathbb{I}_{\{|\zeta_{goal}| \leq \pi/3\}}$, where \mathcal{N} denotes Gaussian distribution with variance σ and β is the amplitude parameter. We set the variance $\sigma = 0.2$ to

ensure that the r_{dist} only includes two narrow reward peaks near the goal and half-way from the goal. Similarly, r_{elev} is defined as $r_{elev} = \mathbb{I}_{\{|\phi| \geq \pi/6\}} \cup \mathbb{I}_{\{|\theta| \geq \pi/6\}}$. Our reward definitions are significantly sparse compared to the traditional dense rewards used in the literature [41].

(a) **Even terrain navigation:** The robot is placed in an obstacle-free even terrain environment and random goals in the range of 10-15 meters away from the starting position given at each episode. The state space is $s = [d_{goal}, \zeta_{goal}]$ and the overall reward formulation $r_{even} = r_{dist} + r_{head}$.

(b) **Uneven terrain navigation:** The robot is placed in an obstacle-free, highly uneven terrain environment. To account for this complexity, we input the roll and pitch of the angle of the robot into the state space, $s = [d_{goal}, \zeta_{goal}, \phi, \theta]$. The objective is to navigate the robot to a goal location along relatively even terrain regions to avoid possible robot flip-overs. The reward is $r_{uneven} = r_{dist} + r_{head} - r_{elev}$.

Terrain	Algorithm	SR (%) \uparrow	PL (# m) \downarrow	EC (m) \downarrow
Even	Reinforce: traj. length = 300 + max entropy	58	22.47	-
	Reinforce: traj. length = 200	32	25.58	-
	Reinforce: traj. length = 300	65	18.75	-
	CCE (Ours)	84	11.62	-
Uneven	Ego-graph [51]	54	20.36	2.189
	Reinforce: traj. length = 300 + max entropy	28	41.32	3.163
	Reinforce: traj. length = 200	8	9.25	3.116
	Reinforce: traj. length = 300	31	32.44	2.236
	CCE (Ours)	72	16.28	1.985

TABLE I: Navigation performance of the policies trained for even and uneven terrain navigation tasks with limited samples. SR denotes success rate, PL denotes average path length, and EC denotes elevation cost. Each method is tested for 100 trials in the outdoor simulator and the average values are reported in the table. CCE has a higher SR, lower PL, and lower EC than baseline approaches in the even terrain, and higher SR and lower EC in uneven. Test environments are different from training environments.

A. Evaluation Metrics for Navigation Paths Generated with Fixed Training Sample Budget

- **Success rate:** The percentage of successful goal-reaching attempts without robot flip-overs (especially in uneven terrain) out of the total number of trials.

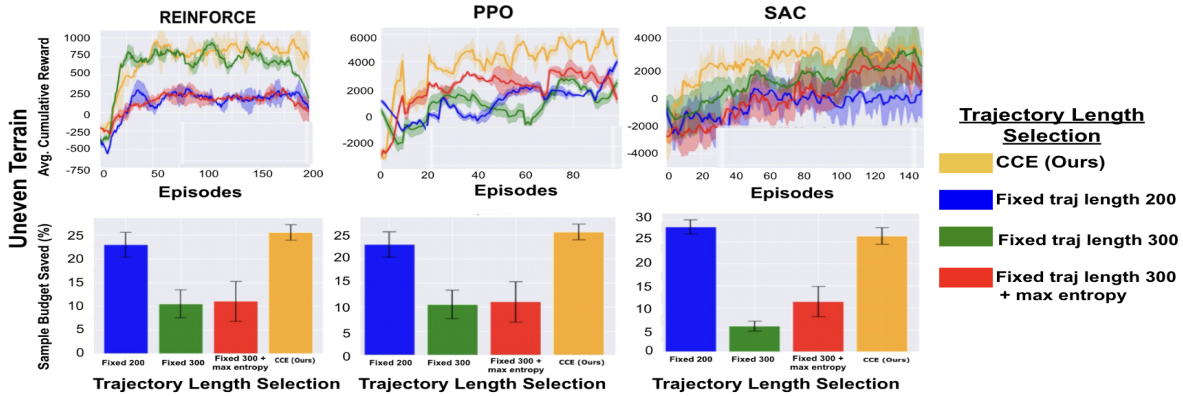


Fig. 6: [TOP] Learning curves during training and [BOTTOM] percent of sample budget ($\sim 4.5e4$) saved during navigation tasks for the uneven terrain (right of Figure 3). Comparison of [LEFT] REINFORCE, [MIDDLE] PPO, and [RIGHT] SAC, with constant and adaptive trajectory lengths. For each algorithm, CCE converges to a higher cumulative reward while expending less of the total budget. We ran 8 to 10 independent replications for each of the 12 experiments. Although a fixed trajectory length of 200 saves the sample budget comparably to CCE, it achieves lower reward in all cases due to the robot flipping over thus causing episodes to end.

- **Average path length:** The average length of path taken to reach goal 10 meters away from the starting position.
- **Elevation cost:** The total elevation gradient experienced by the robot during a trial (i.e., if z_r is the vector that includes the gradient of the vertical motions of the robot along a path, the elevation cost is given by $\|\nabla z_r\|$).

B. Results and Discussions

Policy Learning: We observe in Figure 4 and 6 that, for the outdoor robot simulator, CCE achieves similar or better reward returns with significantly fewer samples under both the navigation settings compared to the fixed trajectory lengths and entropy regularization. Significantly, despite providing comparable returns to CCE, the sample efficiency of the constant and large trajectory lengths is significantly lower (see the bar plots in Fig. 4 and 6). For the agents using CCE, in the even terrain simulations, all agents started with an initial trajectory length of 180, and in the uneven terrain, 200. All those agents end with a final length of 300.

Navigation Performance: We compare our method’s navigation performance qualitatively in Fig. 5 and quantitatively in Table I. To highlight the importance of sample efficiency during training, we use policies trained up to episode 150 for a *limited* sample budget of $\sim 4.5e4$ to perform navigation tasks in even and uneven simulated terrains. The policies, except for ones from CCE, cannot consistently complete the navigation tasks, resulting in significantly lower success rates. Even successful trials of these policies lead to significantly longer paths with several loops instead of heading toward the goal. In contrast, CCE results in relatively straight and consistent paths toward the goals. We further observe that uneven terrain navigation is a comparatively challenging task even for traditional methods such as Ego-graph [51]. Hence, the success rates are relatively low due to the robot flip-overs that occurred during trials. However, CCE leads to higher success rates even compared to baseline methods such as ego-graph. We further observe that CCE results in lower elevation cost indicating that the generated paths are smoother in uneven terrain conditions. Finally, we deploy the

policies trained with the outdoor simulator in the real world using a Clearpath Husky robot. With CCE, even and uneven terrain navigation policies can be transferred to the real world without significant performance degradation in success rate, path length, and elevation cost while other policies show inconsistent performance similar to the simulations.

Remark: Given more training samples, the baseline methods could perform better in success rate and path length during test time given that Figures 4 and 6 show the many times they can reach similar cumulative return as CCE. However, we tested policies from earlier in training to highlight that CCE does not need as many samples.

V. CONCLUSIONS, LIMITATIONS, AND FUTURE WORKS

We propose CCE, which controls exploration and induces training sample efficiency for goal-reaching navigation in the sparse reward setting with RL-based methods by adaptively changing the trajectory length during training. We do so by empirically establishing a positive correlation between a policy’s entropy and the spectral gap of its induced Markov Chain. We show that CCE induces more sample-efficient training than baselines. On real robots, CCE-trained policies generally achieve better success rates and shorter path lengths than ones trained with constant trajectory lengths and entropy regularization for the same sample budget.

A limitation is the scope of our experimental investigation of the connection between policy entropy and the induced spectral gap. Although we cannot explore the connection in complex environments due to spectral gap calculation impracticality, it can still merit investigation for simple environments with continuous state and action spaces. In real-world experiments, policies often lead to high motor vibrations from infeasible velocities provided as actions. Hence, further investigation is required to generate dynamically feasible and smooth actions for better sim-to-real transfer.

REFERENCES

- [1] R. S. Sutton and A. G. Barto, *Reinforcement learning: An introduction*. MIT press, 2018.

- [2] M. Abdeh, F. Abut, and F. Akay, "Autonomous navigation in search and rescue simulated environment using deep reinforcement learning," *Balkan Journal of Electrical and Computer Engineering*, vol. 9, no. 2, pp. 92–98, 2021.
- [3] R. R. Murphy, *Disaster robotics*. MIT press, 2014.
- [4] K. Schilling, "Autonomous navigation of rovers for planetary exploration," *IFAC Proceedings Volumes*, vol. 31, no. 21, pp. 83–87, 1998, 14th IFAC Symposium on Automatic Control in Aerospace 1998, Seoul, Korea, 24–28 August 1998.
- [5] D. Pathak, P. Agrawal, A. A. Efros, and T. Darrell, "Curiosity-driven exploration by self-supervised prediction," in *International conference on machine learning*. PMLR, 2017, pp. 2778–2787.
- [6] S. Chakraborty, A. S. Bedi, A. Koppel, P. Tokekar, and D. Manocha, "Dealing with sparse rewards in continuous control robotics via heavy-tailed policies," *arXiv*, 2022.
- [7] D. Rengarajan, G. Vaidya, A. Sarvesh, D. Kalathil, and S. Shakkottai, "Reinforcement learning with sparse rewards using guidance from offline demonstration," in *International Conference on Learning Representations*, 2021.
- [8] J. Hare, "Dealing with sparse rewards in reinforcement learning," *arXiv preprint arXiv:1910.09281*, 2019.
- [9] C. Wang, J. Wang, J. Wang, and X. Zhang, "Deep-reinforcement-learning-based autonomous uav navigation with sparse rewards," *IEEE Internet of Things Journal*, 02 2020.
- [10] M. Vecerik, T. Hester, J. Scholz, F. Wang, O. Pietquin, B. Piot, N. Heess, T. Rothhölrl, T. Lampe, and M. Riedmiller, "Leveraging demonstrations for deep reinforcement learning on robotics problems with sparse rewards," *arXiv preprint arXiv:1707.08817*, 2017.
- [11] A. S. Bedi, A. Parayil, J. Zhang, M. Wang, and A. Koppel, "On the sample complexity and metastability of heavy-tailed policy search in continuous control," *arXiv preprint arXiv:2106.08414*, 2021.
- [12] T. Haaroja, A. Zhou, P. Abbeel, and S. Levine, "Soft actor-critic: Off-policy maximum entropy deep reinforcement learning with a stochastic actor," in *International conference on machine learning*. PMLR, 2018, pp. 1861–1870.
- [13] N. Botteghi, B. Sirmacek, K. A. Mustafa, M. Poel, and S. Stramigioli, "On reward shaping for mobile robot navigation: A reinforcement learning and slam based approach," *arXiv preprint arXiv:2002.04109*, 2020.
- [14] M. J. Mataric, "Reward functions for accelerated learning," in *Machine Learning Proceedings 1994*, W. W. Cohen and H. Hirsh, Eds. San Francisco (CA): Morgan Kaufmann, 1994, pp. 181–189. [Online]. Available: <https://www.sciencedirect.com/science/article/pii/B9781558603356500301>
- [15] A. Nair, B. McGrew, M. Andrychowicz, W. Zaremba, and P. Abbeel, "Overcoming exploration in reinforcement learning with demonstrations," in *2018 IEEE international conference on robotics and automation (ICRA)*. IEEE, 2018, pp. 6292–6299.
- [16] H.-T. L. Chiang, A. Faust, M. Fiser, and A. Francis, "Learning navigation behaviors end-to-end with autorl," *IEEE Robotics and Automation Letters*, vol. 4, no. 2, pp. 2007–2014, 2019.
- [17] S. Chakraborty, A. S. Bedi, A. Koppel, B. M. Sadler, F. Huang, P. Tokekar, and D. Manocha, "Posterior coresets construction with kernelized stein discrepancy for model-based reinforcement learning," 2023.
- [18] L. Wang, Y. Ling, Z. Yuan, M. Shridhar, C. Bao, Y. Qin, B. Wang, H. Xu, and X. Wang, "Gensim: Generating robotic simulation tasks via large language models," 2024. [Online]. Available: <https://arxiv.org/abs/2310.01361>
- [19] W. A. Suttle, A. Bedi, B. Patel, B. M. Sadler, A. Koppel, and D. Manocha, "Beyond exponentially fast mixing in average-reward reinforcement learning via multi-level monte carlo actor-critic," in *International Conference on Machine Learning*. PMLR, 2023, pp. 33 240–33 267.
- [20] D. J. Hsu, A. Kontorovich, and C. Szepesvári, "Mixing time estimation in reversible markov chains from a single sample path," *CoRR*, vol. abs/1506.02903, 2015.
- [21] G. Wolfer, "Mixing time estimation in ergodic markov chains from a single trajectory with contraction methods," in *Proceedings of the 31st International Conference on Algorithmic Learning Theory*, ser. Proceedings of Machine Learning Research, A. Kontorovich and G. Neu, Eds., vol. 117. PMLR, 08 Feb–11 Feb 2020, pp. 890–905.
- [22] R. J. Williams, "Simple statistical gradient-following algorithms for connectionist reinforcement learning," *Machine learning*, vol. 8, no. 3, pp. 229–256, 1992.
- [23] J. Schulman, F. Wolski, P. Dhariwal, A. Radford, and O. Klimov, "Proximal policy optimization algorithms," *arXiv preprint arXiv:1707.06347*, 2017.
- [24] A. Zai and B. Brown, *Deep reinforcement learning in action*. Manning Publications, 2020.
- [25] R. Houthoofd, X. Chen, Y. Duan, J. Schulman, F. De Turck, and P. Abbeel, "Vime: Variational information maximizing exploration," *Advances in neural information processing systems*, vol. 29, 2016.
- [26] K. Weerakoon, S. Chakraborty, N. Karapetyan, A. J. Sathiamoorthy, A. Bedi, and D. Manocha, "HTRON: Efficient outdoor navigation with sparse rewards via heavy tailed adaptive reinforce algorithm," in *6th Annual Conference on Robot Learning*, 2022.
- [27] A. S. Bedi, S. Chakraborty, A. Parayil, B. M. Sadler, P. Tokekar, and A. Koppel, "On the hidden biases of policy mirror ascent in continuous action spaces," *CoRR*, vol. abs/2201.12332, 2022.
- [28] C. Wang, G. Warnell, and P. Stone, "D-shape: Demonstration-shaped reinforcement learning via goal conditioning," 2023.
- [29] S. Ao, T. Zhou, G. Long, Q. Lu, L. Zhu, and J. Jiang, "Co-pilot: Collaborative planning and reinforcement learning on sub-task curriculum," in *Advances in Neural Information Processing Systems*, M. Ranzato, A. Beygelzimer, Y. Dauphin, P. Liang, and J. W. Vaughan, Eds., vol. 34. Curran Associates, Inc., 2021, pp. 10 444–10 456.
- [30] R. Martinez-Cantin, N. De Freitas, E. Brochu, J. Castellanos, and A. Doucet, "A bayesian exploration-exploitation approach for optimal online sensing and planning with a visually guided mobile robot," *Autonomous Robots*, vol. 27, pp. 93–103, 2009.
- [31] A. Bhatia, P. S. Thomas, and S. Zilberstein, "Adaptive rollout length for model-based rl using model-free deep rl," *arXiv preprint arXiv:2206.02380*, 2022.
- [32] Y. Yao, L. Xiao, Z. An, W. Zhang, and D. Luo, "Sample efficient reinforcement learning via model-ensemble exploration and exploitation," in *2021 IEEE International Conference on Robotics and Automation (ICRA)*. IEEE, 2021, pp. 4202–4208.
- [33] M. Rickert, O. Brock, and A. Knoll, "Balancing exploration and exploitation in motion planning," in *2008 IEEE International Conference on Robotics and Automation*. IEEE, 2008, pp. 2812–2817.
- [34] K. M. B. Lee, F. Kong, R. Cannizzaro, J. L. Palmer, D. Johnson, C. Yoo, and R. Fitch, "An upper confidence bound for simultaneous exploration and exploitation in heterogeneous multi-robot systems," in *2021 IEEE International Conference on Robotics and Automation (ICRA)*. IEEE, 2021, pp. 8685–8691.
- [35] P. Ghassemi and S. Chowdhury, "Decentralized informative path planning with exploration-exploitation balance for swarm robotic search," 2019. [Online]. Available: <https://arxiv.org/abs/1905.09988>
- [36] B. Nakisa, M. N. Rastgoo, and M. J. Norodin, "Balancing exploration and exploitation in particle swarm optimization on search tasking," *Research Journal of Applied Science, Engineering and Technology*, vol. 8, no. 12, pp. 1429–1434, 2014.
- [37] J. Canny, *The complexity of robot motion planning*. MIT press, 1988.
- [38] D. Manocha, *Algebraic and numeric techniques in modeling and robotics*. University of California, Berkeley, 1992.
- [39] S. LaValle, "Planning algorithms," *Cambridge University Press google schola*, vol. 2, pp. 3671–3678, 2006.
- [40] X. Xiao, B. Liu, G. Warnell, and P. Stone, "Motion planning and control for mobile robot navigation using machine learning: a survey," *Autonomous Robots*, pp. 1–29, 2022.
- [41] K. Weerakoon, A. J. Sathiamoorthy, U. Patel, and D. Manocha, "Terp: Reliable planning in uneven outdoor environments using deep reinforcement learning," in *2022 International Conference on Robotics and Automation (ICRA)*, 2022, pp. 9447–9453.
- [42] G. Brunner, O. Richter, Y. Wang, and R. Wattenhofer, "Teaching a machine to read maps with deep reinforcement learning," in *Proceedings of the AAAI Conference on Artificial Intelligence*, vol. 32, no. 1, 2018.
- [43] A. Staroverov, D. A. Yudin, I. Belkin, V. Adeshkin, Y. K. Solomentsev, and A. I. Panov, "Real-time object navigation with deep neural networks and hierarchical reinforcement learning," *IEEE Access*, vol. 8, pp. 195 608–195 621, 2020.
- [44] R. S. Sutton, D. McAllester, S. Singh, and Y. Mansour, "Policy gradient methods for reinforcement learning with function approximation," *Advances in neural information processing systems*, vol. 12, 1999.
- [45] A. S. Bedi, A. Parayil, J. Zhang, M. Wang, and A. Koppel, "On the sample complexity and metastability of heavy-tailed policy search in continuous control," *arXiv preprint arXiv:2106.08414*, 2021.
- [46] R. Dorfman and K. Y. Levy, "Adapting to mixing time in stochastic optimization with Markovian data," in *Proceedings of the 39th International Conference on Machine Learning*, ser. Proceedings of Machine Learning Research, K. Chaudhuri, S. Jegelka, L. Song, C. Szepesvari, G. Niu, and S. Sabato, Eds., vol. 162. PMLR, 17–23 Jul 2022, pp. 5429–5446.
- [47] B. Patel, W. A. Suttle, A. Koppel, V. Aggarwal, B. M. Sadler, A. S. Bedi, and D. Manocha, "Towards global optimality for practical

- average reward reinforcement learning without mixing time oracles,” in *International Conference on Machine Learning*. PMLR, 2024.
- [48] Q. Bai, W. U. Mondal, and V. Aggarwal, “Regret analysis of policy gradient algorithm for infinite horizon average reward markov decision processes,” in *Proceedings of the AAAI Conference on Artificial Intelligence*, vol. 38, no. 10, 2024, pp. 10980–10988.
- [49] D. A. Levin and Y. Peres, *Markov chains and mixing times*. American Mathematical Soc., 2017, vol. 107.
- [50] C. E. Shannon, “A mathematical theory of communication,” *The Bell System Technical Journal*, vol. 27, pp. 379–423, 1948.
- [51] S. Josef and A. Degani, “Deep reinforcement learning for safe local planning of a ground vehicle in unknown rough terrain,” *IEEE Robotics and Automation Letters*, vol. 5, no. 4, pp. 6748–6755, 2020.

A. Experimental Setup Details

Here are the full descriptions of navigation experiments. The first one details the Clearpath Husky simulation experiments in even and uneven terrain shown in the main body. The second one explains the real robotic experiments also shown in the main body. The third set of experiments shows the benefits of CCE with Actor-Critic (AC) in 2D gridworld:

- 1) **Even and Uneven Terrain Navigation in Robotic Simulations:** We use a Unity-based outdoor simulator with a Clearpath Husky robot model to train policies for two navigation tasks: 1. Goal Reaching, 2. Uneven terrain navigation using the Reinforce algorithms. The Unity simulator includes diverse terrains and elevations for training and testing. We restrict ourselves to a $100m \times 100m$ region during training. We used identical policy distribution parameters and neural network architectures with all four algorithms during training and evaluation. The policies are implemented using Pytorch to train in the simulator equipped with a Clearpath Husky robot model, and a ROS Melodic platform. The training and simulations are executed on a workstation with an Intel Xeon 3.6 GHz CPU and an Nvidia Titan GPU. Our agent is a differential drive robot with a two-dimensional continuous action space $a = (v, \omega)$ (i.e. linear and angular velocities). The state space varies for the two navigation tasks and is obtained in real time from the simulated robot’s odometer and IMU sensors. The state inputs used in the two scenarios are,

- $d_{goal} \in [0, 1]$ - Normalized distance (w.r.t the initial straight line distance) between the robot and its goal;
- $\alpha_{goal} \in [0, \pi]$ - Angle between the robot’s heading direction and the goal;
- $(\phi, \theta) \in [0, \pi]$ - Roll and pitch angle of the robot respectively;

Inspired by [26], we define three reward functions: Goal distance reward r_{dist} , Goal heading reward r_{head} , and Elevation reward r_{elev} to formulate the sparse rewards to train our navigation policies. Hence,

$$r_{dist} = \frac{\beta}{2} \mathcal{N}\left(\frac{d_{goal}}{2}, \sigma^2\right) + \beta \mathcal{N}(0, \sigma^2) \quad \text{and, } r_{head} = \mathbb{1}_{\{|\alpha_{goal}| \leq \pi/3\}} \quad (8)$$

where, \mathcal{N} denotes Gaussian distribution with variance σ and β is the amplitude parameter. We set the variance $\sigma = 0.2$ to ensure that the r_{dist} only includes two narrow reward peaks near the goal and half-way from the goal. Similarly, r_{elev} is defines as,

$$r_{elev} = \mathbb{1}_{\{|\phi| \geq \pi/6\}} \cup \mathbb{1}_{\{|\theta| \geq \pi/6\}}. \quad (9)$$

We observe that our reward definitions are significantly sparse compared to the traditional dense rewards used in literature [41].

(a) Even terrain navigation: The robot is placed in an obstacle-free even terrain environment and random goals in the range of 10-15 meters away from the starting position is given at each episode. The state space is $s = [d_{goal}, \alpha_{goal}]$ and the overall reward formulation $r_{even} = r_{goal} + r_{head}$.

(b) Uneven terrain navigation: The robot is placed in an obstacle-free, highly uneven terrain environment. The state space is $s = [d_{goal}, \alpha_{goal}, \phi, \theta]$. The objective is to navigate the robot to a goal location along relatively even terrain regions to avoid possible robot flip overs. The overall reward formulation $r_{uneven} = r_{goal} + r_{head} + r_{elev}$.

- 2) **Real-world Experiments:** The real and simulated testing were conducted in different outdoor scenarios. Particularly, the real-world environments are reasonably different in terms of terrain structure(i.e. elevation gradient) and surface properties(i.e grass and tiny gravel regions with different levels of friction) which are not included or modeled in the simulator (e.g. elevation gain in the simulator is up to $\sim 4m$, however, we restricted it to $\sim 1.5m$ elevation gain in the real world for robot’s safety). Our Clearpath Husky robot is equipped with a VLP16 LiDAR and a laptop with an Intel i9 CPU and an Nvidia RTX 2080 GPU.
- 3) **Increasing Obstacles in 2D gridworld:** Agent starts at the top left of a 25-by-25 grid and navigates to the bottom right. The agent can move up, down, left, right, or stay. It gains a reward of +1 for reaching the goal and +0 otherwise. We have three different gridworlds: one with no obstacles and two with walls. If the agent takes an action that would cause it to collide with a wall, it will just stay in its current location. We use Actor-Critic method and compare against fixed trajectory length and randomly-sampled trajectory length (MAC) [19]. Because of the state and action space are both discrete, our implementation involves using a linear approximator for each state-action pair and then a softmax operation for the actor and another linear approximator for each state for the critic.

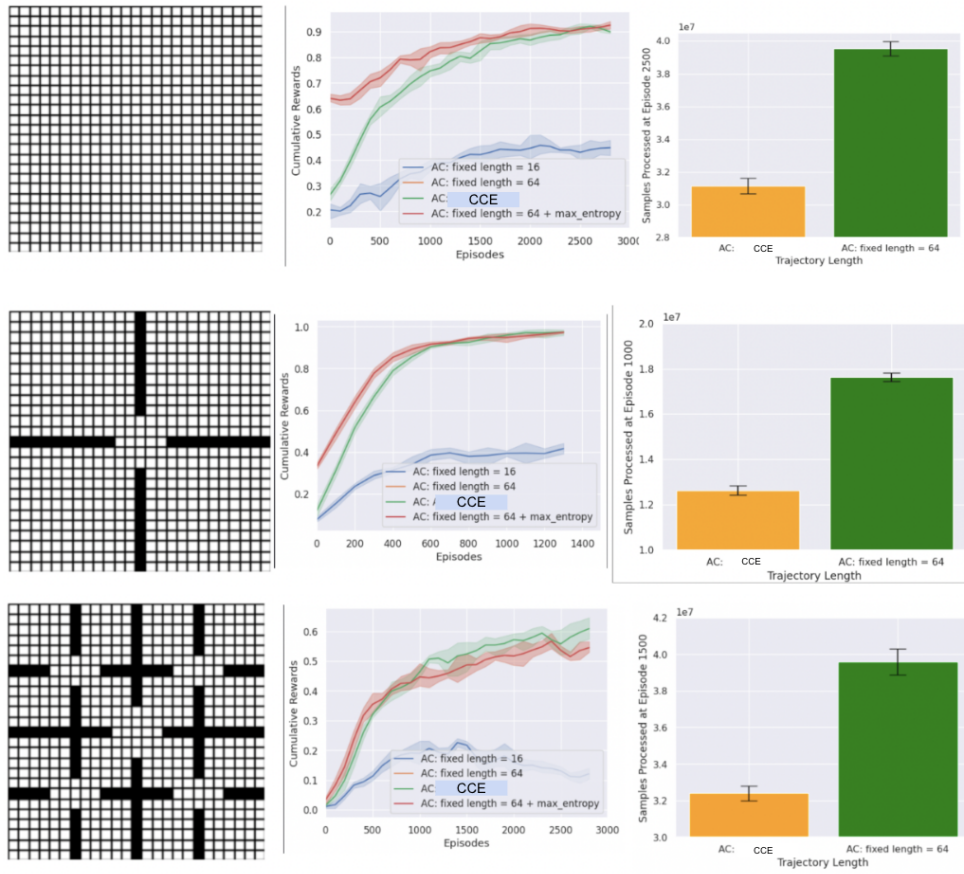


Fig. 7: 25-by-25 gridworld environments with Actor-Critic with constant and adaptive trajectory and constant trajectory with max-entropy regularization for learning navigation to bottom right. [LEFT] Visualization of the grid environment where white represents open space and black represents walls. [MIDDLE] The mean cumulative rewards over 2500 episodes. [RIGHT] The number of samples processed between adaptive length and constant length 64.

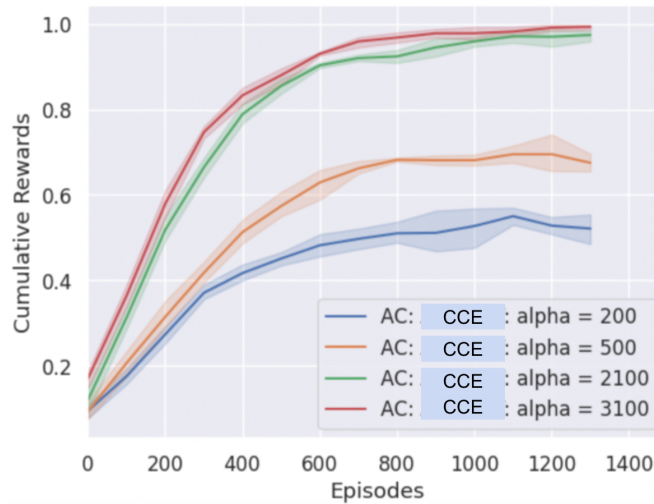


Fig. 8: We train CCE models in the 4 wall environment with changing values of α for five trials each. The t_i for all models is 16. We see that as α decreases, the RL agents converge to suboptimal rewards.

To show that other monotonic transformations between policy entropy and trajectory length can be used, we trained another AC model for five trials with CCE trajectory selection scheme using an exponential mapping:

$$t_c = f(H_c) = \text{round}(t_i e^{\alpha(\frac{H_c}{H_i} - 1)}) \quad (10)$$

Figure 9 shows the training with exponential transformation compared against linear transformation given in Eq 7 and fixed trajectory lengths. We see that the exponential transformation is the most sample efficient.

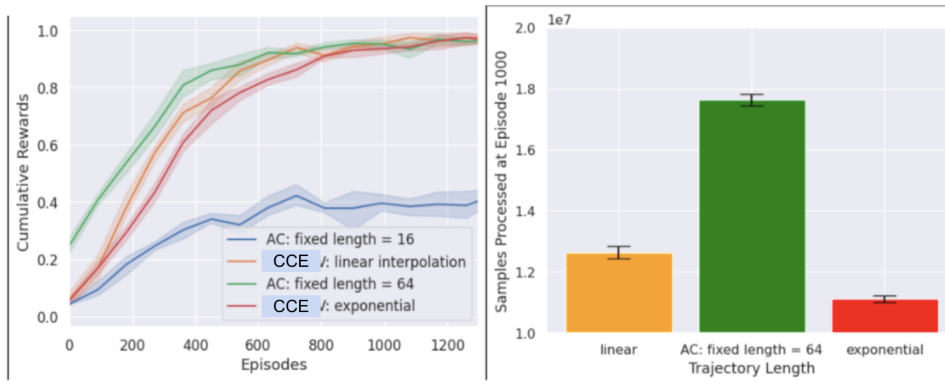


Fig. 9: Training plot in the 4 walls environments with AC. We train two models with CCE selection scheme: one with linear transformation given in Eq 7 and one with exponential given in Eq 10

TABLE II: This table compares the hyperparameters and performance between the four experiments, each run for five trials

Environment	Model	Trajectory Method	α	Trajectory Change	Learning Rate	No. of Iterations Per Episode
2D Gridworld						
No Obstacles	AC	Fixed = 16			0.01	500
No Obstacles	AC	Fixed = 64			0.01	500
No Obstacles	AC	CCE	1100	16 \rightarrow 56	0.01	500
No Obstacles	AC + max-entropy	Fixed = 64			0.01	500
4 Walls	AC	Fixed = 16			0.01	500
4 Walls	AC	Fixed = 64			0.01	500
4 Walls	AC	CCE	2100	16 \rightarrow 61	0.01	500
4 Walls	AC + max-entropy	Fixed = 64			0.01	500
16 Walls	AC	Fixed = 16			0.01	500
16 Walls	AC	Fixed = 64			0.01	500
16 Walls	AC	CCE	2100	16 \rightarrow 69	0.01	500
16 Walls	AC + max-entropy	Fixed = 64			0.01	500
Robot Simulations						
Even Terrain	REINFORCE	Fixed = 200			0.0001	400
	REINFORCE	Fixed = 300			0.0001	400
	REINFORCE	CCE	3200	180 \rightarrow 300	0.0001	400
	REINFORCE	Fixed = 300 + max entropy			0.0001	400
Uneven Terrain	REINFORCE	Fixed = 200			0.0001	400
	REINFORCE	Fixed = 300			0.0001	400
	REINFORCE	CCE	3200	200 \rightarrow 300	0.0001	400
	REINFORCE	Fixed = 300 + max entropy			0.0001	400
Even Terrain	PPO	Fixed = 200			0.0005	400
	PPO	Fixed = 300			0.0005	400
	PPO	CCE	3200	180 \rightarrow 300	0.0005	400
	PPO	Fixed = 300 + max entropy			0.0005	400
Uneven Terrain	PPO	Fixed = 200			0.0005	400
	PPO	Fixed = 300			0.0005	400
	PPO	CCE	3200	200 \rightarrow 300	0.0005	400
	PPO	Fixed = 300 + max entropy			0.0005	400
Even Terrain	SAC	Fixed = 200			0.0003	400
	SAC	Fixed = 300			0.0003	400
	SAC	CCE	3200	180 \rightarrow 300	0.0003	400
	SAC	Fixed = 300 + max entropy			0.0003	400
Uneven Terrain	SAC	Fixed = 200			0.0003	400
	SAC	Fixed = 300			0.0003	400
	SAC	CCE	3200	200 \rightarrow 300	0.0003	400
	SAC	Fixed = 300 + max entropy			0.0003	400